Comparing tractive performance of steel and rubber single grouser shoe under different soil moisture contents

Ge Jun[1], Wang Xiulun[1,2*], Koji Kito[1]

(1. *Graduate School of Bioresources, Mie University, Tsu 514-8507, Japan*;
2. *College of Engineering, Anhui Agricultural University, Hefei 230036, China*)

Abstract: Steel and rubber are two kinds of materials which are often used for the tracks of off-road vehicles. The objective of this study was to compare tractive performances of steel and rubber grouser shoes under different soil moisture contents. In this study, the tractive performance of single grouser shoe was predicted by soil parameters and three-dimensional shearing model. The soil used in this study was clay soil, and ten different soil moisture contents ranged from 8.58% to 54.36% were applied for investigation of soil parameters. For each soil moisture content, the penetration test, direct shearing test, density and soil moisture content measurement have been performed to obtain the required soil parameters. The experimental results showed that thrust and running resistance of steel single grouser shoe had similar trends to those of rubber single grouser shoe. The thrust of rubber single grouser shoe was always greater than that of steel single grouser shoe with the increase of soil moisture content, and as well as the running resistance. However, the traction of rubber single grouser shoe had a different trend to that of steel single grouser shoe. The traction of steel single grouser shoe was always greater than that of rubber single grouser shoe at any given moisture content except at the stage of less than 15% moisture content. From the experimental results, it can be concluded that the steel single grouser shoe performed better than rubber single grouser shoe in traction for the soil used in this study.

Keywords: steel grouser shoe, rubber grouser shoe, soil moisture content, tractive performance, running resistance, tracked vehicle

DOI: 10.3965/j.ijabe.20160902.1688

Citation: Ge J, Wang X L, Kito K. Comparing tractive performance of steel and rubber single grouser shoe under different soil moisture contents. Int J Agric & Biol Eng, 2016; 9(2): 11－20.

1 Introduction

Off-road vehicles have a wide range of applications, such as agriculture, exploration, construction, mining, military[1-3]. The improvement of traction performance is significant for vehicle mobility[4,5]. Since Bekker[6], who worked for US Army Waterways Experiment Station, used the cone index to assess vehicle mobility and terrain trafficability on a "go/no go" basis, the research field of terramechanics has been developing for more than half a century. Wong et al.[7,8] also did a lot of theoretical research and made practical applications such as the introduction of the theory of terramechanics and off-road vehicles, the research of high-mobility tracked vehicles for over snow operations, and study on predicting the performances of rigid rover wheels on extraterrestrial surfaces based on test results obtained on earth. There are other researchers who also have made great advances regarding vehicle tractive performance. Grisso et al.[4] proposed mathematical models for predicting tractive performance of rubber-tracks in agricultural soils; Li et al.[5] have carried out a study that focused on the development of an algorithm to calculate the tractive capacity of an off-road vehicle with stochastic vehicle

Received date: 2015-01-15 **Accepted date:** 2016-01-16

Biographies: Ge Jun, PhD student, Research interests: terramechanics, Email: gejun.mieu@aliyun.com; **Koji Kito**, PhD, Associate Professor, Research interests: Energy Utilization Engineering, Email: kito@bio.mie-u.ac.jp.

∗**Corresponding author: Wang Xiulun**, PhD, Professor, Research interests: energy utilization engineering, Graduate School of Bioresources, Mie University, Japan. Tel: +81 059-231-9594, Email: wang@bio.mie-u.ac.jp.

parameters (such as suspension stiffness, suspension damping coefficient, tire stiffness, and tire inflation pressure), operating on soft soil with an uncertain level of moisture, and on a terrain topology that induces rapidly changing external excitations on the vehicle; Lyasko et al.[9,10] had done research on the effect of multi-pass on off-road vehicle tractive performance and slip sinkage effect in soil-vehicle mechanics.

Tractive performance of off-road wheeled and tracked vehicles is significantly affected by soil conditions. Furthermore, it mainly depends on the shearing and sinkage characteristics of soil[1,6]. Since the interaction between an off-road vehicle and the terrain is complex and difficult to model accurately[11], the empirical methods for predicting a vehicle's tractive performance have been developed[12]. Gill et al.[13] pointed out that soil and its conditions greatly influence traction, the soil mechanic is very complex and direct measurement for force of wheel/track-soil interaction is very difficult, so most of the equations for predicting traction performance have been empirically developed. Since Bekker et al.[6] used the cone index to predict the vehicle mobility and terrain trafficability, many methods ranging from theoretical to empirical were proposed for predicting and measuring vehicle traction performance. Wong et al.[12] introduced a similar approach to estimate the tractive effort developed by the lugs (grouser) of a cage wheel, such as that used in paddy fields or that attached to a tire as a traction-aid device on wet soils. In an another study, Park et al.[14] describe a mathematical model designed to allow for the determination of the mechanical relationship existing between soil characteristics and the primary design factors of a tracked vehicle, and to predict the tractive performance of this tracked vehicle on soft terrain. The material which is usually used for tracks of off-road vehicles is steel or rubber or the two materials combined together. Wong et al.[15] had also compared wheels and tracks of off-road vehicles based on the tractive performance. However, he focused on the shape of the running gear rather than the influence of soil moisture content.

In this study, the authors used two kinds of material, rubber and steel, to predict the tractive performance of a single grouser shoe, and comparing the performance influenced by the two materials. There are many parameters for describing the dynamic properties of soil, so the tests such as direct shearing test, penetration test were performed to derive the required parameters. The test soil was clay soil, and ten different moisture contents were changed by adding water into the soil. The tests were repeated when the moisture content changed. When the experiments were all completed and the soil parameters were all obtained, the fitted curves were graphed respectively. Subsequently, the three-dimensional (3D) shearing model was used for predicting tractive performance of steel and rubber single grouser shoe. Finally, the different performances of steel and rubber single grouser shoes were compared.

2 Theoretical framework

When the tire or the sprocket of a track is applied by a torque, shearing action takes place on the vehicle running gear-terrain interface, as shown in Figure 1[12].

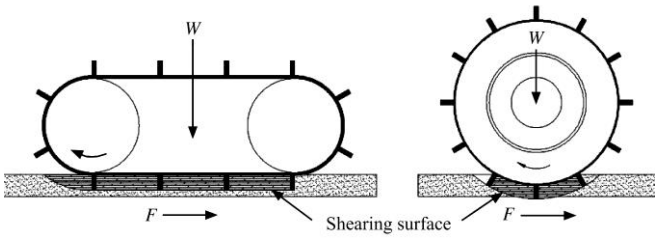

Figure 1 Shearing action of a track and a wheel

Tracked vehicles such as bulldozers which need a large amount of traction are usually equipped with grouser shoe as running gear[16]. This study focused on single grouser shoe and the single grouser shoe model as shown in Figure 2 was adopted. In order to compare the difference of tractive performance of single grouser shoe using steel and rubber at different soil moisture contents, it is necessary to predict the thrust generated by single grouser shoe, and for this purpose, the shearing status beneath grouser shoe has to be known. Many soil failure types beneath grouser shoe could be considered including but not necessarily limited to the arc of a circle and a logarithmic spiral. In this study, 3D shearing model was proposed as soil shearing failure model shown in Figure 3. The forces acting on 3D shearing model are shown in Figure 4. From this figure, it is clear that

the single grouser shoe is loaded by W in a vertical direction. Equilibrium equation of vertical forces could be expressed as follow:

$$W = L(k_c + Bk_\varphi)\{\lambda(h+Z_0)^n + (1-\lambda)Z_0{}^n\} \quad (1)$$

where, L is the shoe pitch, cm; B is the width of single grouser shoe, cm; h is the height of grouser, cm; λ is the ratio of grouser thickness to shoe pitch; k_c is the cohesion modulus in Bekker's equation, kgf/cm^{n+1}; k_φ is friction modulus in Bekker's equation, kgf/cm^{n+2}; n is the exponent of sinkage in Bekker's equation; Z_0 is the sinkage of single grouser shoe, cm.

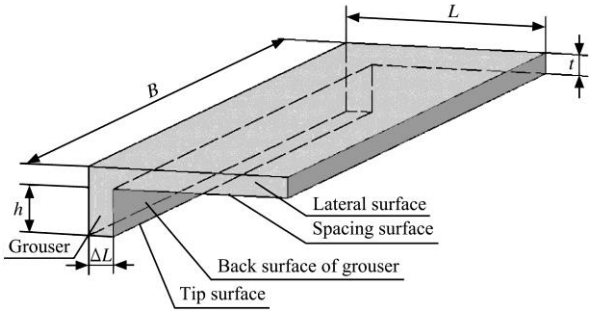

Figure 2 Single grouser shoe model

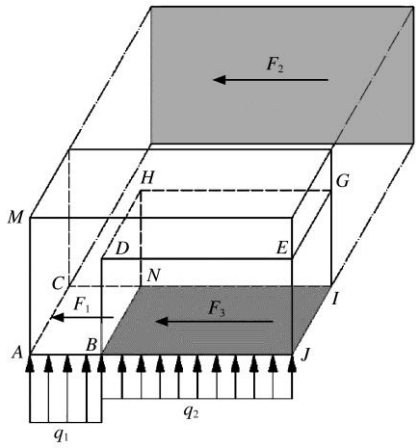

Figure 3 Three-dimensional shearing model

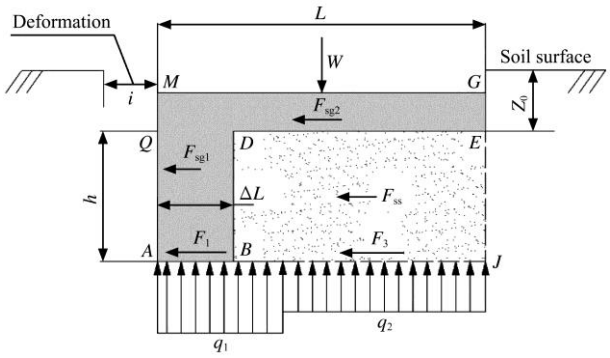

Figure 4 Forces act on shearing model

From the Figure 4, thrust F consists of three forces: F_1, F_2 and F_3. F_1 is the shearing force generated by grouser tip surface, and expressed in Equation (2); F_2 is the force of both lateral sides includes grouser shoe and soil beneath spacing surface of shoe which moves together with the moving of grouser shoe, and it is consists of F_{sg1}, F_{sg2} and F_{ss}, (the expressions of them are shown in Equations (3), (4) and (5) respectively); F_3 is the shearing force generated by the soil's bottom surface (surface BJIN in Figure 3), and the expression is shown in Equation (6):

$$F_1 = \lambda LB(C_a + q_1 \tan\delta) \quad (2)$$

where, C_a is the soil adhesion, kPa; q_1 is the pressure on grouser tip surface, kPa; δ is the soil external friction angle, degree.

$$F_{sg1} = 2\lambda hL\left[C_a + \tan\delta\tan\left(45-\varphi/2\right)\left\{\frac{\gamma_t(2Z_0+h)}{2}\tan\left(45-\varphi/2\right)-2C\right\}\right] \quad (3)$$

where, φ is the soil internal friction angle, degree; and γ_t is the soil density, kg/m^3; C is soil cohesion, kPa.

$$F_{sg2} = \begin{cases} 2Z_0L\left[C_a + \tan\delta\tan\left(45-\varphi/2\right)\left\{\frac{\gamma_t Z_0}{2}\tan\left(45-\varphi/2\right)-2C\right\}\right] & Z_0 \le t \\ 2tL\left[C_a + \tan\delta\tan(45-\varphi/2)\left\{\frac{\gamma_t(2Z_0-t)}{2}\tan(45-\varphi/2)-2C\right\}\right] & Z_0 \ge t \end{cases} \quad (4)$$

where, t is the thickness of shoe spacing, cm.

$$F_{ss} = \left[C + \tan^2\left(45-\varphi/2\right)\tan\varphi\left\{q_3 + \gamma_t\left(h+2Z_0\right)/2\right\} - 2C\tan\left(45-\varphi/2\right)\tan\varphi\right] \quad (5)$$

where, q_3 is the pressure on spacing surface of shoe (surface DEGH in Figure 3), kPa.

$$F_3 = (1-\lambda)LB(C + q_2\tan\varphi) \quad (6)$$

where, q_2 is the pressure on soil failure surface (surface BJIN in Figure 3), kPa.

The thrust force F is resultant of F_1, F_2 and F_3, and could be expressed as follows:

$$F = F_1 + F_2 + F_3 = F_1 + 2(F_{sg1} + F_{sg2} + F_{ss}) + F_3 \quad (7)$$

The running resistance R could be expressed as Equation (8):

$$R=\frac{k_c+Bk_\varphi}{n+1}\{(h+Z_0)^{(n+1)}\lambda+Z_0^{(n+1)}(1-\lambda)\} \quad (8)$$

Obviously, traction of grouser shoe P could be expressed in Equation (9):

$$P=F-R \quad (9)$$

3 Experimental conditions

In this study, a clay soil, whose plastic limit is 40.1% and liquid limit is 48.5%, was used as the test soil. The soil condition was altered by changing the soil moisture content by the addition of water into the soil. Ten different moisture contents (dry base) were applied for this experiment: 8.6%, 12.5%, 17.2%, 22.3%, 27.7%, 28.9%, 34.2%, 39.4%, 47.0% and 54.4%.

Traditionally, the cone penetrometer technique, the bevameter technique and traditional technique of civil engineering soil mechanics are used for measuring the mechanical properties of soil[1,17]. For this study, the soil parameters which were required for predicting tractive performance need to be investigated. More specifically, modulus k_c, k_φ and n could be obtained by penetration test; soil cohesion, soil adhesion, soil internal friction angle and external friction angle could be derived by direct shearing test; soil density and moisture content should be measured during each experiment. The entire process of the experiment is shown as Figure 5.

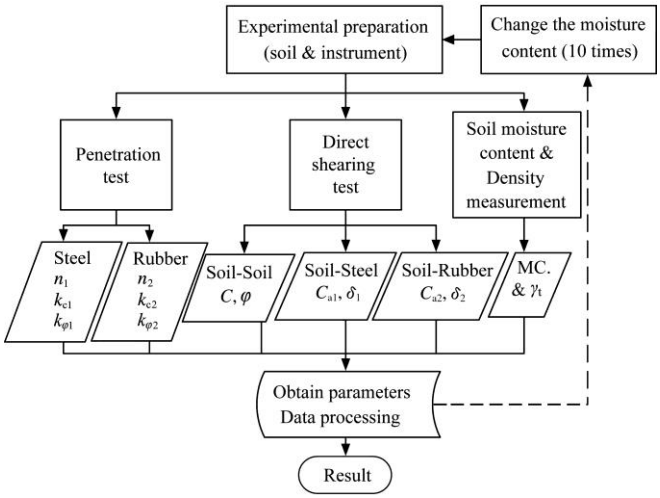

Figure 5 Experimental process

According to the flow chart, the test soil needs to be prepared first. The raw field soil was dried in the sun and mesh screened with a 2 mm sieve. After experimental preparation, the penetration test, direct shearing test, density and soil moisture content measurement were carried out to obtain the soil parameters which were required for this study. After completing the tests for one soil moisture content, certain amount of water base on the experimental plan was added to the soil to change the moisture content. In order to know soil parameters of this moisture content soil, the process which was used in soil of previous moisture content was repeated until the tenth soil moisture content. Finally, the obtained parameters will be used for predicting tractive performance of single grouser shoe.

3.1 Penetration test and test device

The penetration test is the measurement of normal pressure-sinkage relationship. If test soil is considered to be homogeneous within the depth of interest, its pressure-sinkage relationship could be characterized by the following Equation (10) which proposed by Bekker[4]:

$$q=(k_c/b+k_\varphi)Z_0^n \quad (10)$$

where, q is normal pressure, kPa; b is the smaller side of test plate, cm.

There are two steel plates and two rubber plates used in this experiment. For one material, the length of plates is 3.0 cm and the width of plates is 1.9 cm and 2.5 cm. The values of k_{c1}, $k_{\varphi1}$ and n_1 can be derived from the results of steel plates. The values of k_{c2}, $k_{\varphi2}$ and n_2 can be derived from the results of rubber plates.

The penetration tester used in this experiment is shown in Figure 6.

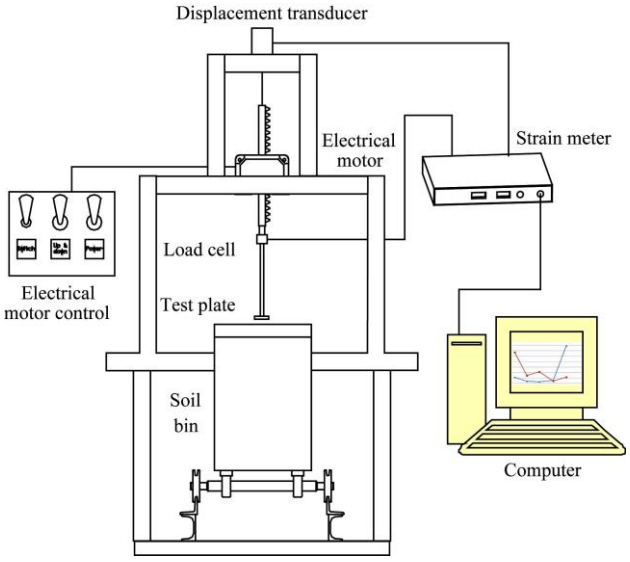

Figure 6 Penetration tester device

The schematic diagram as shown in Figure 6 is the penetration test device which was used for this study.

Based on the figure, a soil bin with the dimensions of 24.5 cm × 40 cm × 100 cm was used for penetration test, and the penetration power is provided by an electrical motor which is assembled together with a spur rack. The displacement of test plate and the pressure acting on test plate when test is ongoing was measured by load cell and displacement transducer, respectively. At the same time, the data obtained by load cell and displacement transducer is recorded by an A/D converter interface which is connected to a computer. For each material, there are two different plates used in this test and the dimensions are 1.9 cm×3.0 cm and 2.5 cm×3.0 cm. For each test plate, the penetration test was performed twice in every soil moisture contents. According to the result of this test, the modulus in Equation (10) was realized. A locale photo was shot that shows in Figure 7.

Figure 7 Locale photo of penetration tester device

3.2 Direct shearing test and test device

In this study, the shearing test was carried out using the direct shearing device. The schematic diagram of the apparatus is shown in Figure 7. The device essentially consists of power unit, a shearing box and sensors for monitoring shearing force and displacement. In this study, the upper shearing box was always filled with clay soil, and the lower shearing box was filled with soil or materials such as steel and rubber.

When the two boxes was filled with soil sample for measuring soil cohesion and internal friction angle, soil cohesion and internal friction angle can be expressed as Equation (11).

$$\tau = C + \sigma \tan\varphi \tag{11}$$

where, τ is shearing stress, kPa; σ is vertical pressure, kPa.

When the lower box was filled with steel or rubber, soil adhesion and external friction angle can be measured and showed in Equation (12):

$$\tau = C_a + \sigma \tan\varphi \tag{12}$$

As shown in Figure 8, the lower shearing box is pushed by a screw stem which is driven by an electrical motor. When the shearing is taking place, the shearing force is measured by a load cell and the shearing displacement is measured by a potentiometer. Both sensors are connected to a strain meter, and then signals are delivered to a computer for processing.

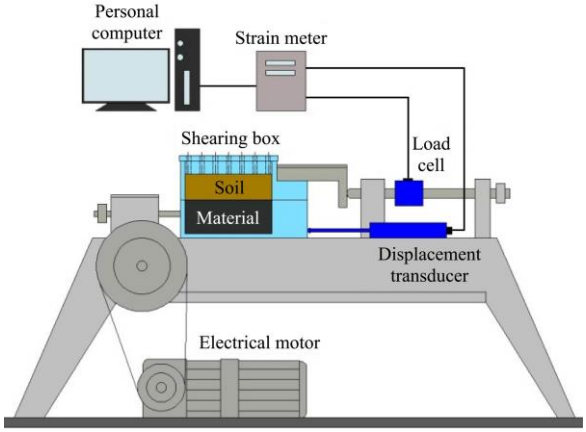

Figure 8 Soil shearing test device

3.3 Dimension of single grouser shoe and vertical load

After the soil parameters have been obtained, predictions of thrust, running resistance and traction of single grouser shoe were conducted. In the prediction, dimension of single grouser shoe such as pitch of shoe, width of shoe, spacing thickness, grouser height and ratio of grouser thickness to shoe pith was fixed, as shown in Table 1. During the experiment, the vertical load on the single grouser shoe was constant.

Table 1 Dimension of single grouser shoe and vertical load

Item	Specific content
Pitch of shoe (L)/cm	9
Width of shoe (B)/cm	15
Thickness of spacing/cm	3
Height of grouser (h)/cm	3
Ratio of grouser thickness to shoe pitch (λ)	0.1
Vertical load (W)/kg	22.5

4 Results and discussion

4.1 Soil parameters result

Penetration test, direct shearing test, density

measurement for ten levels of soil moisture contents were completed. Soil parameters were determined. In order to investigate the relationships among soil cohesion, adhesion and moisture content, the soil cohesion and soil adhesion for steel and rubber are graphed in Figure 9.

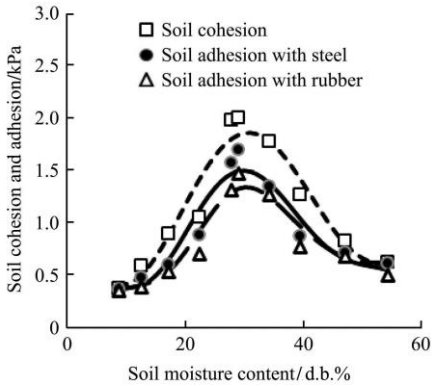

Figure 9 Soil cohesion and adhesion

Figure 9 indicates the relationships among soil cohesion, soil adhesion and moisture content. From this figure, soil adhesions with steel and rubber have the similar trend to on another. Soil cohesion and adhesion were all small when the soil moisture content was low, and then increased with the increase of moisture content until the respective peak values. After that, they began to decrease with the increase of soil moisture content to a low value when the soil moisture content was high. From the figure, soil cohesion and soil adhesion at low moisture content were smaller than those at high moisture content, respectively. Basically, for any given moisture content, the soil cohesion was greater than soil adhesion, and soil adhesion with steel was greater than that with rubber except when the moisture content was less than 15% or higher than 45%.

Figure 10 shows the soil internal friction angle and external friction angles.

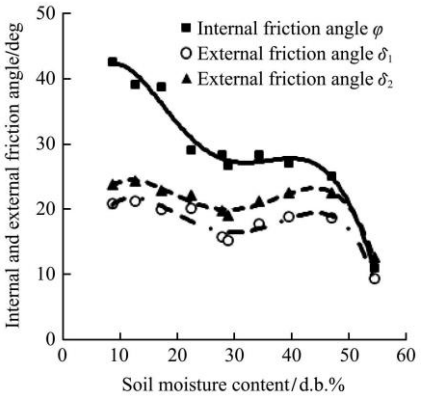

Figure 10 Internal and external friction angle

Figure 10 indicates that the internal friction angle decreased with the increase of soil moisture content except for the middle section from about 30% to 40% which barely changed. When the moisture content was low, the internal friction angle was large. However, because of the decrease, the internal friction angle approached that of the external friction angles when the moisture content was higher than 48%. Meanwhile, the fitting curves for soil external friction angles with steel and rubber were almost parallel, but the external friction angle of soil to rubber was always greater than the external friction angle of soil to steel. When the soil moisture content was low, the external friction angles increased with the increase of soil moisture content, this then began to decrease until the trough value, and they then increased to the second peak value. After that, they continuously decreased with the increase of soil moisture content. As the results show, external friction angles did not vary significantly before 48% moisture content.

The modulus k_c of steel and rubber plates has been graphed in Figure 11.

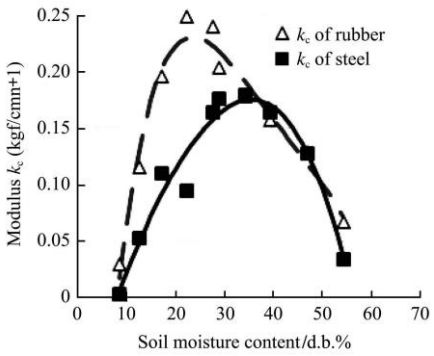

Figure 11 Modulus k_c

Figure 11 shows the relationship among the modulus k_c's results of steel test plate, rubber test plate and moisture content. From the figure, it could know that k_c of steel test plate have similar trend to that of rubber test plate. k_c is a modulus which is concerned with soil cohesion, so both k_c of steel and rubber test plate were very small when the moisture content was low. They increased with the increase of moisture content until the peak values, and after that they decreased with the increase of moisture content. However, the k_c of these two materials' test plate have some differences such as when the test plate was rubber, the peak value of k_c emerged at 23% of moisture content rather than that of

steel which was at 35%, and prior to 35% moisture content, k_c of rubber test plate was greater than k_c of steel test plate.

Figure 12 is the modulus k_φ of steel and rubber test plates.

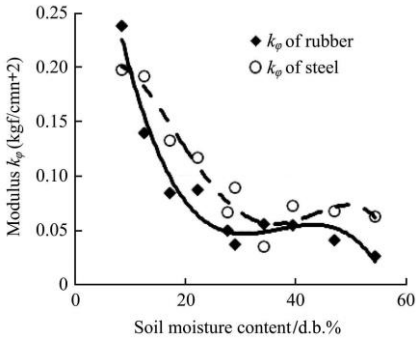

Figure 12 Modulus k_φ

Figure 12 shows the modulus k_φ determined for steel and rubber test plates. k_φ of the rubber test plate showed a similar trend to k_φ of the steel test plate, much like that of modulus k_c. k_φ is a modulus concerned with friction, so k_φ of the two material's test plate have high values when the moisture content was low, and then they decreased with the increase of moisture content. After that, both of them barely changed with the increase of moisture content. Although the trends both materials' k_φ were similar, some differences existed. At first, when the moisture content was low, the k_φ of the rubber test plate was greater than that of the steel test plate. However, after a moisture content of 10%, k_φ of rubber test plate was always smaller than that of steel test plate at any given moisture content.

The sinkage exponent of steel and rubber test plates is shown in Figure 13.

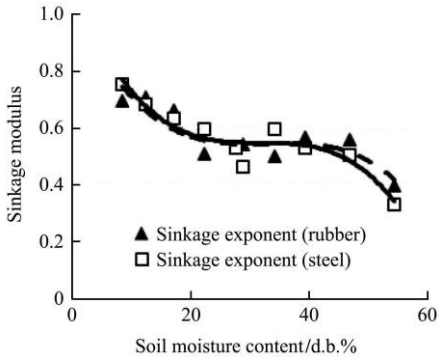

Figure 13 Sinkage exponent

Figure 13 indicates the sinkage exponent used for the steel and rubber test plates. Obviously, the sinkage exponent moduli used for steel and rubber test plates have similar trends with each other. When the moisture content was low at first, the sinkage exponents of both materials had their maximum values. They both subsequently decreased with the increase of soil moisture content, with the exception of the middle section of moisture content from 25% to 40% in which the moduli were almost unchanged. For these two sinkage exponents, some differences existed between them even though they were close to each other. Before 35% of moisture content, the sinkage exponent of the steel test plate was greater than that of rubber test plate, but after 35% of moisture content, the situation reversed.

The variation of soil density is shown in Figure 14.

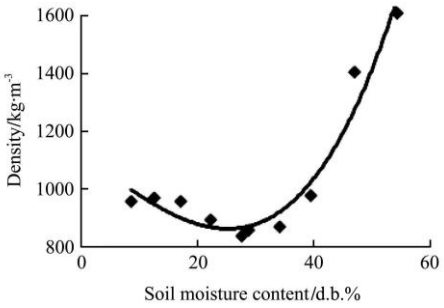

Figure 14 Soil density

Figure 14 shows the result of soil density and fitting curve for it. From the figure, the density decreased with the increase of moisture content until it reached a trough value, and then it increased rapidly with the increase of soil moisture content. However, one can easily observe that the density did not vary significantly from 8.5% to 40% of moisture content, and then begin to rapidly increase until the maximum value of density. This is because of the volume swelling when the water added into the test soil only lightly changed the densities. Conversely, after 40% of soil moisture content, when the water was added into the soil to obtain the highest soil moisture content, the forms of soil changed from a semi-solid to a fluid state, and at the same time the volume of soil shrunk because of capillary forces.

4.2 Prediction results and discussion

In this study, the soil moisture content which was used for predicting tractive performance changed from 8.5% to 53%. The soil parameters could be obtained by respective fitting curves which were discussed above.

The materials used for single grouser shoe were steel and rubber in this study. After prediction of tractive performance, the relationship between tractive performance of two materials' single grouser shoes and moisture content was determined.

The relationships among thrust of two materials' single grouser shoes and soil moisture content was graphed as Figure 15.

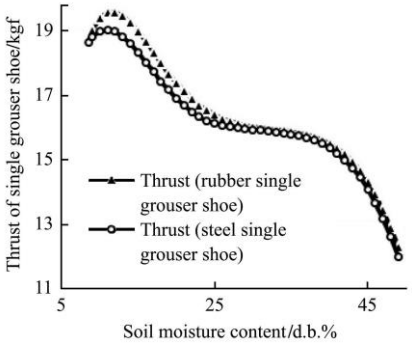

Figure 15 Relationships among thrusts of steel single grouser shoe, rubber single grouser shoe and soil moisture content

From this figure, the thrusts of steel and rubber single grouser shoes have a similar trend and are close to each other. They both decreased with the increase of soil moisture content except at low soil moisture content, where the thrusts increased to peak value, respectively. Compared to the thrusts at other soil moisture contents, the thrusts have mild variations when soil moisture content was from 25% to 36%. However, the thrust of rubber single grouser shoe was always greater than that of steel single grouser shoe at any given soil moisture content. As mentioned in Equation (7), the thrust of single grouser shoe is the resultant of 3D model's shearing forces generated by grouser tip surface, both lateral sides and the soil bottom surface. Because the grouser thickness ratio λ was 0.1, the shearing force generated by grouser tip surface was small. Compared to pressure in vertical direction, pressure on the lateral side was smaller which caused the shearing force generated by both lateral sides to be small as well. The thrust was mainly determined by the soil bottom surface. When the moisture content was high, the thrust of both materials' single grouser shoe rapidly decreased with the increase of moisture content. The reason is that the parameters such as friction angle, k_c, k_φ, and n all decreased with the increase of the moisture content.

The relationship between running resistance of two materials' single grouser shoes and moisture content is showed in Figure 16 as follows.

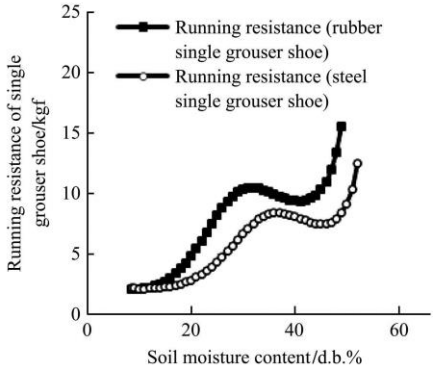

Figure 16 Relationships among running resistances of steel single grouser shoe, rubber single grouser shoe and soil moisture content

Figure 16 indicates that running resistances of steel and rubber single grouser shoe have more complex trends than that of thrusts. Running resistances of steel and rubber single grouser shoe have a similar trend to each other in the way that they changed with the soil moisture content. When the soil moisture content was low at first, the resistances of steel and rubber single grouser shoe were almost equal to each other, and then they increased with the increase of soil moisture content until their respective peak values. After that, both of them began to decrease with the increase of soil moisture content to their respective trough values. Finally, they increased rapidly with the increase of soil moisture content when the moisture content was at a high level. The sinkage increase that resulted in the increase of resistance and running resistance largely depends on the sinkage of the grouser shoe. As further increase of soil moisture content, the modulus k_φ was increased and the modulus k_c was still in a relatively high value (as shown in Figures 11 and 12) which caused the sinkage of grouser shoe to decrease. In other words, the resistance also decreased with the increase of soil moisture content precisely as this figure shows. This is because k_c, k_φ and n were all decreased to a small value and the test soil was turned to a liquid state when the soil moisture content was high. All of these made it hard to support the single grouser shoe anymore and caused a rapid increase of sinkage. Obviously, differences also exist between the resistances

of steel and rubber single grouser shoes. The resistance of rubber single grouser shoe was greater than that of steel single grouser shoe at any given moisture content. For the rate of increase before the respective peak value, the resistance of rubber grouser shoe was much faster than that of steel single grouser shoe. The soil moisture content while resistance of rubber single grouser shoe was at its peak value was about 5% lower than that of steel. This was also true when the soil moisture contents were at their trough values.

Since the thrust and running resistance of rubber and steel single grouser shoe have been predicted, the traction of two material's single grouser shoe can be determined. The relationship between traction and soil moisture content has been graphed and shown in Figure 17.

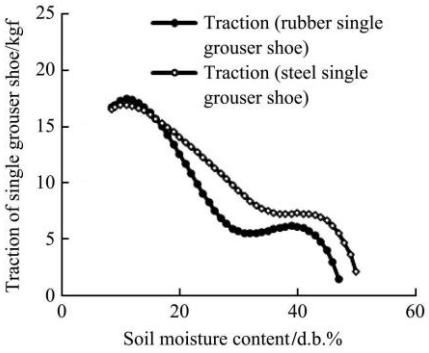

Figure 17 Relationships among tractions of steel single grouser shoe, rubber single grouser shoe and soil moisture content

Traction is the difference of thrust to running resistance of single grouser shoe. Because thrust was much greater than resistance when the soil moisture content was low at first, traction was mainly determined by the thrust and it was the reason that the tractions minimally increased at low soil moisture content. With the increase of soil moisture content, the traction of steel single grouser shoe continuously decreased until the maximum soil moisture content. However, when the soil moisture content ranged from 35% to 45%, the traction of the steel single grouser shoe barely changed with the increase of soil moisture content. Meanwhile, the traction of the rubber single grouser shoe decreased with the increase of soil moisture content until the trough value of 5.2 kgf at 31% soil moisture content. After the trough value, the traction of rubber single grouser shoe increased with the increase of soil moisture content until the second peak value of 6 kgf at 40% soil moisture content. When the soil moisture content further increased, it began to decrease again with the increase of soil moisture content until the highest moisture content. One can see that when the soil moisture content was at a high level, the tractions of both the steel and rubber single grouser shoes rapidly decreased with the increase of soil moisture content. The reasons for that are the rapid decrease of thrust as shown in Figure 15 and the rapid increase of resistance as shown in Figure 16. From this figure, the traction of steel single grouser shoe was always greater than that of rubber single grouser shoe at any given soil moisture content except the stage of less than 15% soil moisture content. Generally speaking, the steel single grouser shoe performed better than the rubber single grouser shoe for the soil used in this study.

5 Conclusions

In this study, in order to predict tractive performance of single grouser shoe, the required soil parameters should be known. Ten different levels of soil moisture content have been changed for test soil by adding water to it. The penetration test and direct shearing test have been carried out for each soil moisture content. In order to compare the difference of tractive performance of steel and rubber single grouser shoe at different soil moisture contents, the 3D shearing model was proposed. From this study, it could be concluded as follows:

1) The experimental results showed that the soil parameters changed with the variation of the soil moisture content even though the soil had the same constituents with the exception of water.

2) According to the prediction results of tractive performance, traction shows a better performance when the soil moisture content was at a low level no matter which material was used for the single grouser shoe. That means it is better that tracked vehicles operate under the soil condition of a relative low moisture content level.

3) From the result of this study, the steel single grouser shoe showed a better traction performance than the rubber single grouser shoe when grouser height was 3 cm, the ratio of grouser thickness to shoe pitch was 0.1 and the soil was clay soil.

[References]

[1] Wong J Y. Terramechanics and off road vehicle engineering: Terrain behavior, off-road vehicle performance and design. 2nd ed. UK: Elsevier; 2010.

[2] Senatore C, Sandu C. Off-road tire modeling and the multi-pass effect for vehicle dynamics simulation. Journal of Terramechanics, 2011; 48(4): 265–276.

[3] Wang X L, Yamazaki M, Tanaka T. Dynamic behavior of an open lugged wheel under paddy soil conditions. Journal of Terramechanics, 1993; 30(3): 191–203.

[4] Grisso R, Perumpral J, Zoz F. An empirical model for tractive performance of rubber-tracks in agricultural soils. Journal of Terramechanics, 2006; 43(2): 225–236.

[5] Li L, Sandu C. On the impact of cargo weight, vehicle parameters, and terrain characteristics on the prediction of traction for off-road vehicles. Journal of Terramechanics, 2007; 44(3): 221–238.

[6] Bekker M G. Introduction to terrain-vehicle systems. Ann Arbor: The University of Michigan Press; 1969.

[7] Wong J Y. Development of high-mobility tracked vehicles for over snow operations. Journal of Terramechanics, 2009; 46(4): 141–155.

[8] Wong J Y. Predicting the performances of rigid rover wheels on extraterrestrial surfaces based on test results obtained on earth. Journal of Terramechanics, 2012; 49(1): 49–61.

[9] Lyasko M. Multi-pass effect on off-road vehicle tractive performance. Journal of Terramechanics, 2010; 47(5): 275–294.

[10] Lyasko M. Slip sinkage effect in soil-vehicle mechanics. Journal of Terramechanics, 2010; 47(1): 21–31.

[11] Abo-Elnor M, Hamilton R, Boyle J T. Simulation of soil–blade interaction for sandy soil using advanced 3D finite element analysis. Soil & Tillage Research, 2004; 75(1): 61–73.

[12] Wong J Y. Theory of ground vehicles. 3rd ed. New York: John Wiley& Sons; 2001.

[13] Gill W R, Vanden Berg G E. Soil dynamics in tillage and traction. Agricultural Handbook, No. 316, U.S. Government Printing Office, Washington, D.C. 1967; 512 p.

[14] Park W Y, Chang Y C, Lee S S, Hong J H, Park J G, Lee K S. Prediction of the tractive performance of a flexible tracked vehicle. Journal of Terramechanics; 2008; 45(1-2): 13–23.

[15] Wong J Y, Huang W. "Wheels vs. tracks"–A fundamental evaluation from the traction perspective. Journal of Terramechanics, 2006; 43(1): 27–42.

[16] Tsuji T, Nakagawa Y, Matsumoto N, Kadono Y, Takayama T, Tanaka T. 3-D DEM simulation of cohesive soil-pushing behavior by bulldozer blade. Journal of Terramechanics, 2012; 49(1): 37–47.

[17] Wang X L, Sato K, Ito N, Kito K, Hasegawa S, Garcia P P. Tangential adhesion using glass beads and a glass plate. Journal of JSAM, 2005; 67(6): 89–94.